reactivity of olefinic substrates that have the possibility of alternative reaction pathways and associated products. Such reactions will be carried out with the acylperoxo complexes, $[Cu_2(XYL\text{-}O\text{-})(OOR)]^{2+}$,[37] since these do react with olefins.[38]

Thus, $[Cu_2(XYL\text{-}O\text{-})(OOH)]^{2+}$ (**3**) does not appear to display exceptional reactivity toward organic substrates and we suggest that this can be ascribed to the fact that the coordinated hydroperoxo group is bound simultaneously to two Cu(II) ions, in an environment that is essentially coordinatively saturated and that has limited steric accessibility to substrate molecules. Degradative processes, either hydroperoxide disproportionation or reactions of $(Cu_2(XYL\text{-}O\text{-})(OOH)]^{2+}$ (**3**) with solvent, are also clearly important and in competition with processes involving substrate oxidation.

Summary

Transition-metal hydroperoxo species are well established as important intermediates in the oxidation of hydrocarbons,[4] and a number of recent studies have focused upon the isolation of such complexes and studies of their reactivity.[45e,51] Here, we have reported on one of the first examples of a hydroperoxo complex of copper, $[Cu_2(XYL\text{-}O\text{-})(OOH)]^{2+}$ (**3**), containing a μ-1,1-hydroperoxo (^-OOH) ligand. A Cu^{II}–OOH complex generated by the one-electron reduction and protonation of a superoxo–Cu(II) compound, $LCu^{II}\text{-}(O_2^-)$,[42b,c] has also recently been described.[52]

In copper biochemistry, a Cu–OOH species has been implicated by Klinman and co-workers[53] as an important intermediate in the reaction of the copper monooxygenase, dopamine β-hydroxylase. It is suggested that the reduction of O_2 at a Cu(I) center is accompanied by a proton transfer from a protein-derived group leading to the copper–hydroperoxo intermediate. This is then capable of abstracting a hydrogen atom from the benzyl dopamine substrate and subsequent oxygen atom transfer leads to products. A Cu–OOH moiety has also been proposed to be involved in the disproportionation of superoxide ($2O_2^- + 2H^+ \rightarrow O_2 + H_2O_2$) mediated by the copper–zinc superoxide dismutase (SOD) enzyme.[54,55] Since an Fe–OOH intermediate has been suggested in the oxidation of the tetrahydropterin cofactor in phenylalanine hydroxylase,[56] further descriptions of the action of the copper-dependent form of the enzyme[15b] may require the consideration of a Cu–OOH species, by analogy.

Porphyrin–M–OOR and other Fe–OOR complexes have come under recent scrutiny because of their relevance to the active oxygenating reagent in cytochrome P-450 monooxygenase.[47] In synthetic systems, powerful M–(O) oxidizing agents form from M–OOR intermediates via heterolytic and/or homolytic O–O cleavage processes.[47] In the enzyme it seems likely that protonation of an $Fe\text{–}O_2$ intermediate similarly leads to the active iron–oxo reagent. We expect that related effects may be seen in copper ion chemistry, and we are continuing to study the reactivity of both mononuclear and dinuclear Cu_n–OOR species.

Acknowledgment. We thank the National Institutes of Health (K.D.K.) and the Science and Engineering Research Council of the UK (N.J.B.) for their generous support of this research. We thank the Daresbury Laboratory for use of facilities and provision of beam time. We also thank the NATO Scientific Affairs Bureau for the award of a travel grant (RG.82/0139) to N.J.B. and K.D.K.

Supplementary Material Available: ORTEP diagram of the complete cation of **6b** and tables of bond lengths, bond angles, anisotropic temperature factors, and hydrogen coordinates and temperature factors for **6b** (Tables VI–IX) (11 pages); listing of structure factors (Table V) (36 pages). Ordering information is given on any current masthead page.

(51) Also see, for example, (a) Saussine, L.; Brazi, E.; Robina, A.; Mimoun, H.; Fischer, J.; Weiss, R. *J. Am. Chem. Soc.* **1985**, *107*, 3534. (b) Sugimoto, H.; Sawyer, D. T. *J. Am. Chem. Soc.* **1985**, *107*, 5712. (c) Sugimoto, H.; Sawyer, D. T. *J. Org. Chem.* **1985**, *50*, 1784–1786. (d) Durand, R. R., Jr.; Bencosme, C. S.; Collman, J. P.; Anson, F. C. *J. Am. Chem. Soc.* **1983**, *105*, 2710. (e) Strukul, G.; Michelin, R. A. *J. Am. Chem. Soc.* **1985**, *107*, 7563–7569. (f) Francis, K. D.; Cummins, D.; Oakes, J. *J. Chem. Soc., Dalton Trans.* **1985**, 493. (g) Ledon, H. J.; Varescon, F. *Inorg. Chem.* **1984**, *23*, 2735–2737.

(52) (a) Thompson, J. S., personal communication. (b) Thompson, J. S. *Recl. Trav. Chim. Pays-Bas* **1987**, *106*(6-7), 354.

(53) Miller, S. M.; Klinman, J. P. *Biochemistry* **1985**, *24*, 2114–2127.

(54) Osman, R.; Basch, H. *J. Am. Chem. Soc.* **1984**, *106*, 5710–5714.

(55) Rosi, M.; Sgamellotti, A.; Tarantelli, F.; Bertini, I.; Luchinat, C. *Inorg. Chem.* **1986**, *25*, 1005–1008.

(56) Dix, T. A.; Benkovic, S. J. *Biochemistry* **1985**, *24*, 5839–5846.

Cobalt(II)-Facilitated Transport of Dioxygen in a Polystyrene Membrane

M. J. Barnes, R. S. Drago,* and K. J. Balkus, Jr.

Contribution from the Department of Chemistry, University of Florida, Gainesville, Florida 32611. *Received March 21, 1988*

Abstract: In this paper we present conclusive evidence to illustrate that reversible binding of O_2 to transition-metal O_2 carriers can be utilized to facilitate transport of O_2 through a solid membrane when such complexes are incorporated into the membrane. The key experiment to establish this concept involves the proper selection of a blank film. The polystyrene-supported CoSDPT type complexes and blanks consisting of nickel(II) derivatives are ideal for demonstrating facilitated transport because of their structural similarity. We also present a procedure for evaluating permeation data, which should find widespread use in this area since it eliminates imperfections that can exist in test and blank membranes. A transport mechanism is discussed in light of these results.

The separation of oxygen and nitrogen is of industrial significance for the production of pure oxygen and pure nitrogen. The main commercial processes for oxygen production involve cryogenic air separation[1] and pressure swing adsorption.[2] Many applications do not require high-purity oxygen but can use oxygen-enriched air. This market includes waste-water treatment facilities, the pulp and paper industry, fermentation processes, and numerous medical applications. To produce lower purity oxygen

(1) (a) Barron, R. F. *Cryogenic Systems*, 2nd ed.; Oxford University: New York, 1985. (b) Hands, B. A. *Cryogenic Engineering*; Academic: London, 1986. (c) Braton, N. R. *Cryogenic Recycling and Processing*; CRC: Boca Raton, FL, 1980.

(2) (a) Knoblauch, K. *Chem. Eng. (N.Y.)* **1978**, *85*, 87. (b) Miwa, K.; Inoue, T. CEER, *Chem. Econ. Eng. Rev.* **1980**, *12*, 40. (c) Whyte, T. E., Jr.; Yon, C. M.; Wagener, E. H. *Industrial Gas Separations*; ACS Symposium Series 223; American Chemical Society: Washington, DC, 1983.

0002-7863/88/1510-6780$01.50/0

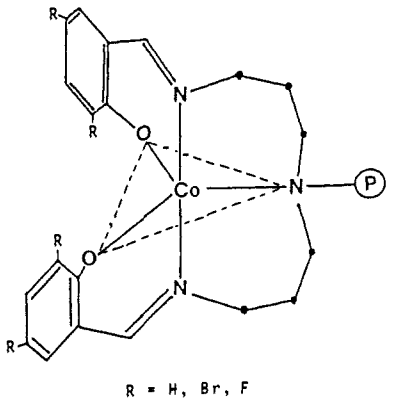

Figure 1. Polystyrene-bound CoSDPT (SDPT = bis((salicylidene-amino)propyl)amine).

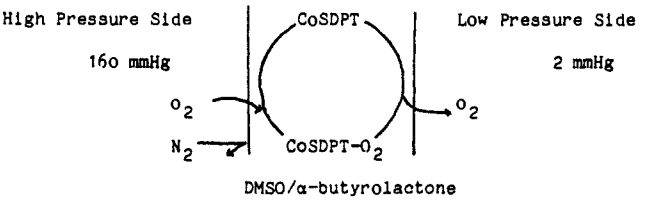

Figure 2. Bend Research liquid-membrane oxygen-enrichment process.

or pure nitrogen, selective-gas permeation[2c,3] through a polymer membrane provides an alternative separation method, which is becoming increasingly more important.

Ideally, both high selectivity and flux as well as good mechanical strength are desirable for a permselective polymer membrane. The incorporation of additives to modify permeation properties has been directed toward improving membranes that are highly permeable and poorly selective. A recent approach to this concept involves enhancing the transport of dioxygen by encapsulating a metal complex containing solution in a porous polymer membrane resulting in excellent selectivity.[4] This liquid-membrane, oxygen-enrichment process utilizes cobalt(II) chelate complexes. The best example cited was for [*N*,*N*'-bis(salicylideneamino)di-*n*-propylamine]cobalt(II), CoSDPT (Figure 1, with Ⓟ replaced by H), in 1:1 DMSO and α-butyrolactone solvent encapsulated in a 130-μm thick microporous nylon 6,6 membrane.[5] At 25 °C, an air mixture containing 88% oxygen was produced in a single pass through this membrane. This system is depicted in Figure 2. Although the process appears quite remarkable, the removal of the volatile solvent by gas flow hinders its commercial development. A few reports of the facilitated transport of oxygen by carriers in membranes has appeared,[6] using unsupported complexes that can be viewed as being dissolved in the polymer.

The results presented in this paper represent a new approach to enhancing the permeation properties of polymer membranes and establish a novel method and mechanism of transport. A metal complex that reversibly binds dioxygen is covalently attached to polystyrene. Though the pure complexes in the solid state do not bind O_2, they do bind oxygen in the solid state when covalently linked to a solid polymer.[7] The dispersion of the metal complex

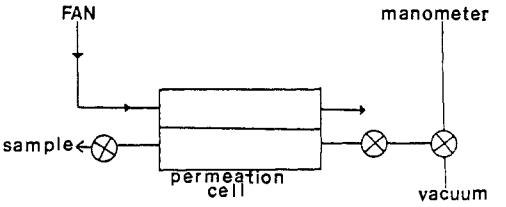

Figure 3. Schematic diagram of the gas-permeation experimental setup.

on highly cross-linked polystyrene into a polystyrene film resulted in the selective permeation of O_2 through the membrane. This membrane system differs from the liquid membranes in that the metal complexes are bound to the polymer. Since the cobalt complexes are not mobile, the mechanism is unlike that proposed for isotropic polymers or liquid membranes.

Recently, our system has been extended to cobalt(II) porphyrin and Schiff base complexes.[8] In all reports[6,8] of facilitated transport in solid polymer membranes including our recent communication,[9] the demonstration of facilitated transport by metal complex binding of O_2 is dependent upon the critical selection of a blank. Incorporation of a material in a polymer film can function to change the structure of the membrane and the permeability of gases leading to enrichment by a process other than facilitated transport. The results of this study are significant for they provide strong support for a facilitated transfer mechanism using metal complexes to bind simple gas molecules. A procedure for the evaluation of the experimental permeation data is reported that eliminates imperfections including solvent entrapment that surely exist in the test and blank films.

Experimental Section

Permeation Apparatus. The apparatus, previously described,[9] was designed to provide meaningful data in the simplest way, while allowing for support of the membrane under experimental permeation conditions. A schematic representation of the entire permeation setup is shown in Figure 3.

Permeation Procedure. A typical permeation experiment would be conducted as follows. A polymer membrane is secured between the two chambers of the apparatus. After a period of time has elapsed in which the membrane has deformed to the shape of the O-rings used to secure its seal, a vacuum is applied. The lower chamber is typically evacuated for $^1/_2$ h to remove any excess solvent or O_2 that may have been trapped in the film during its preparation. Pumping is then stopped, and an initial pressure reading is taken of the closed system. Gas samples of the lower chamber were taken with a 100-μL gas-tight syringe and analyzed by a Varian 3700 gas chromatograph equipped with a thermal conductivity detector. The column employed was an 8-ft, $^1/_8$-in.-o.d., stainless-steel column containing 5-Å molecular sieves heated to 30 °C.

Since the gas sample taken is at a reduced pressure, it is diluted with air as it is withdrawn from the sampling port. From the percent oxygen of the injected sample determined by the GC, the actual percent oxygen in the lower chamber can be determined by eq 1, where P_L is the pressure

$$P_L O_L + (P_H - P_L) O_H = P_H O_D \quad (1)$$

of the lower chamber (mmHg), P_H is atmospheric pressure, O_L is the percent oxygen in the lower chamber, O_H is the percent oxygen in the atmosphere, and O_D is the percent oxygen as determined by the GC. The standard deviation between samples was typically on the order of 0.1%.

Membrane Preparation. The membranes employed in this study were prepared by a casting technique. Polystyrene was dissolved in an appropriate solvent, most often toluene or methylene chloride. The viscous polymer solution was then poured onto a leveled glass plate. Evaporation of solvent at room temperature resulted in the formation of uniform polymer membranes.

Membranes containing the supported metal complexes were prepared in a similar manner. The solid supported complexes were ground to a fine powder (<1 μm in diameter) and then added to the polymer solution. The weight percent of the amount of added complex is determined after

(3) (a) Stern, S. A.; Frisch, H. L. *Annu. Rev. Mater. Sci.* **1981**, *11*, 523. (b) Meares, P. *Membrane Separation Processes*; Elsevier: Amsterdam, The Netherlands, 1976. (c) Lloyd, D. R. *Materials Science of Synthetic Membranes*; ACS Symposium Series 269; American Chemical Society: Washington, DC, 1985.

(4) (a) Schultz, J. S.; Soddard, J. D.; Suchdeo, S. R. *AIChE J.* **1974**, *20*, 417. (b) Smith, D. R.; Lander, R. J.; Quinn, J. A. *Recent Dev. Sep. Sci.* **1977**, *3*, 225. (c) Way, J. D.; Noble, R. D.; Flynn, T. M.; Sloan, E. D. *J. Membr. Sci.* **1982**, *12*, 239. (d) Kimura, S. G.; Matson, S. L.; Ward, W. J., III *Recent Dev. Sep. Sci.* **1979**, *5*, 11.

(5) Roman, I. C.; Baker, R. W. U.S. Patent No. 4542010, 1985.

(6) (a) Sterzel, H. J.; Sanner, A. Ger. Offen. DE No. 3407149, 1985, *Chem. Abstr.* **1986**, *104*, 110951j. (b) Nishide, H.; Kuwahara, M.; Ohyanagi, M.; Funada, Y.; Kawakami, H.; Tsuchida, E. *Chem. Lett.* **1986**, 43.

(7) Drago, R. S.; Gaul, J. H.; Zombeck, A.; Straub, D. K. *J. Am. Chem. Soc.* **1980**, *102*, 1033.

(8) (a) Nishide, H.; Ohyanagi, M.; Okada, O.; Tsuchida, E. *Macromolecules* **1986**, *19*, 494. (b) Nishide, H.; Ohyanagi, M.; Okada, O.; Tsuchida, E. *Macromolecules* **1987**, *20*, 417. (c) Tsuchida, E.; Nishide, H.; Ohyanagi, M.; Kawakami, H. *Macromolecules* **1987**, *20*, 1907. (d) Nishide, H.; Ohyanagi, M.; Kawakami, H.; Tsuchida, E. *Bull. Chem. Soc. Jpn.* **1986**, *59*, 3213.

(9) Drago, R. S.; Balkus, K. J., Jr. *Inorg. Chem.* **1986**, *25*, 716.

Table I. Permeation Data for PS/[P]–CoSDPT (16.4%) Membrane

time, h	total pressure, mmHg	flux, mmHg/h	partial pressure, mmHg		% oxygen	% enrichment
			oxygen	nitrogen		
5	36.0	7.20	10.56	25.44	29.3	8.3
18	71.0	3.94	23.77	47.23	33.5	12.5
24	92.0	3.83	29.78	62.22	32.4	11.4
29.5	99	3.35	32.97	66.03	33.3	12.3
42	118	2.81	40.27	77.73	34.1	13.1

the permeation experiment by redissolving the polymer film, filtering the added supported complex, drying, and weighing.

Membrane Characterization. The membrane thickness was determined with a vernier caliper to the nearest 0.01 mm.

Polystyrene-Supported Dipropylenetriamine, [P]–DPT. Polystyrene beads (90% chloromethylated, 4% divinylbenzene cross-linked) were donated by Sybron Corp. Polystyrene-bound dipropylenetriamine was prepared according to the literature.[7]

Polystyrene-Supported Bis[3-(salicylideneamino)propyl]amine, [P]–SDPT. The polymer-bound pentadentate ligand was prepared according to the literature.[7] The 3,5-dibromo- and the 3-fluoro-substituted salicylaldehyde derivatives were prepared in a similar manner.

[P]–CoSDPT, –$CoBr_2$SDPT, and –Co3FSDPT. Cobalt was incorporated into the SDPT ligands by slurrying excess cobalt(II) acetate with the resins in DMF under argon at room temperature for 2 days. The polymer-supported cobalt complexes were suction filtered, washed with DMF, and dried under vacuum at 80 °C. Analysis of [P]–CoSDPT indicated >95% of the chloromethylated polystyrene had been converted to the [P]–SDPT and that 1.15% of the SDPT ligand contained cobalt. This low loading of cobalt was viewed as ideal for this study because site isolation inhibits formation of the μ-peroxo dimer. EPR studies showed an intense cobalt–dioxygen signal, which was used to monitor reversible binding of O_2.

[P]–NiSDPT and –$NiBr_2$SDPT. The analogous nickel complexes were prepared in the same manner as reported for the cobalt complexes.

Silica Gel Supported CoSDPT, $CoBr_2$SDPT, and Co3FSDPT. Silica gel supported dipropylenetriamine was prepared as reported in the literature.[10] The silica gel supported Co^{II}SDPT complexes were prepared from [SG]–DPT in an analogous manner to the polystyrene-bound analogues.

Results and Discussion

The evaluation of the cobalt-containing membranes is based upon a comparison of experimental permeation data with data from an appropriate blank. Permeation data for a typical PS/[P]–CoSDPT membrane is shown in Table I. The percent oxygen was calculated as previously described, and the percent enrichment is the difference between the percentage of oxygen in the lower chamber and air, as determined by gas chromatography. Permeation is a first-order kinetic process:

$$\frac{dP}{dt} = \frac{RTA}{22414V_{cell}} \frac{\bar{P}(P_H - P_L)}{l}$$

where $\bar{P}$ = permeability coefficient (cm^3 (STP)·cm/cm^2·s·mmHg), l = film thickness (cm), A = film area (cm^2), V_{cell} = volume of the lower chamber (cm^3), $P_H - P_L$ = partial pressure differential across the membrane (mmHg), R = gas constant (6.24×10^4 cm^3·mmHg/mol·K), and T = temperature (K). With P_H constant, we obtain eq 2. The constant represents the intercept of ln ($P_H - P_L$) at time zero. A plot of ln ($P_H - P_L$) versus time should yield a straight line, indicating a first-order process. The analysis of the lower chamber for oxygen and nitrogen partial pressure leads to the permeability coefficients for oxygen (Figure 4) and nitrogen obtained from the slope of the lines obtained by treating the partial pressures with eq 2. Values of 4.38×10^{-10} and 1.92×10^{-10} are obtained, respectively.

$$\ln (P_H - P_L) = \frac{-RTA}{22414V_{cell}} \frac{\bar{P}}{l} t + \text{constant} \qquad (2)$$

In the cobalt complex containing films, oxygen transport through the membrane does not follow a first-order process.

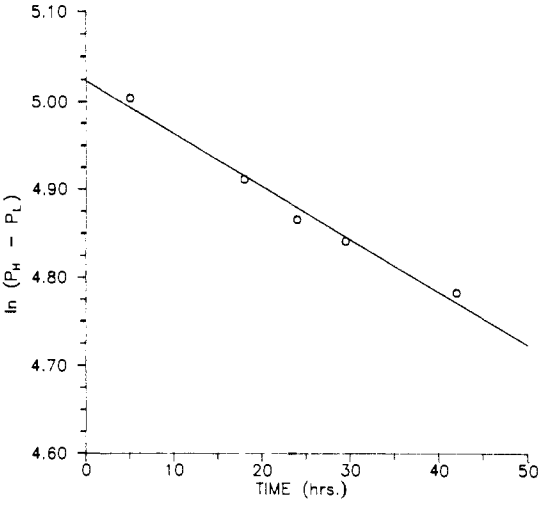

Figure 4. Plot of the natural log of the oxygen pressure differential across the membrane as a function of time for PS/[P]–CoSDPT (16.4%).

Instead, a slightly curved line is obtained, indicating that the permeability coefficient of oxygen is varying with the partial pressure of oxygen in the lower chamber.

Certainly, all films contained minor defects, some more severe than others. An extensive amount of data was collected on a large number of films. In several instances pinholes were present in the original film or leaks developed as the experiment progressed. In order for a run to be found acceptable, we required that the first data point have as an upper limit a value of flux times length (l), below 7.0 Torr·mm/h at the start of the experiment. The second requirement was that in each experiment the flux must decrease as $P_H - P_L$ decreases, i.e., as time increases. This criteria was used to discard data sets in which leaks developed during the experiment. A series of 11 films of polystyrene with varying thickness were studied yielding a mean O_2 permeability coefficient of 3.1×10^{-10} cm^3 (STP)·cm/(cm^2·s·mmHg) with a standard deviation of $\pm 0.8 \times 10^{-10}$. This permeability coefficient is approximately 1 order of magnitude greater than those previously reported.[11] This is not surprising since polystyrene is a glassy polymer and the method of membrane preparation affects the transport properties of the membrane.[12] Systematic errors introduced by the apparatus or sampling technique may also contribute to the deviation. Our permeabilities were also determined from a gas mixture rather than a single-component gas penetrating through the membrane. The few studies reported with permeations of gas mixtures through glassy polymers show deviations in permeabilities of pure penetrants versus those in the mixture.[13] For our purposes, the important point is that all films were made and evaluated in a similar manner so that consistent data could be obtained. Using $\bar{P}_{N_2}$ as an internal standard ensures that the cobalt complex containing membranes can be compared with their respective blanks, and the difference in O_2 partial pressures attributed to metal-promoted enhanced-O_2 permeability and not to film preparation or defects.

In order to demonstrate facilitated transport, the cobalt-containing films must be compared to an appropriate blank. Analogous nickel(II) complexes do not bind O_2 and are similar in structure to the cobalt(II) complexes, resulting in membranes with similar free space volumes. Although free volume is difficult to reproduce in glassy-filled polymers because of trapped air

(10) Pribich, D. C. Ph.D. Dissertation, University of Florida, 1985.

(11) (a) Paterson, C. M. *J. Appl. Polym. Sci.* **1968**, *12*, 2649. (b) Yashuda, H.; Rosengren, K. J. *J. Appl. Polym. Sci.* **1970**, *14*, 2839. (c) Salame, M. *J. Polym. Sci.* **1973**, *41*, d1. (d) Stannett, V. T. *Polym. Eng. Sci.* **1978**, *18*, 1129. (e) Kawakami, Y.; Karasawa, H.; Kamiya, H.; Aoki, T.; Yamashita, Y. *Polym. J. (Tokyo)* **1986**, *18*, 237.

(12) (a) Carre, A.; Gamet, D.; Schultz, J.; Schreiber, H. P. *J. Macromol. Sci., Chem.* **1986**, *A23*, 1. (b) Chainey, M.; Wilkinson, M. C.; Hearn, J. *J. Polym. Sci.* **1985**, *23*, 2947.

(13) Chern, R. T. Ph.D. Dissertation, North Carolina State University, 1983.

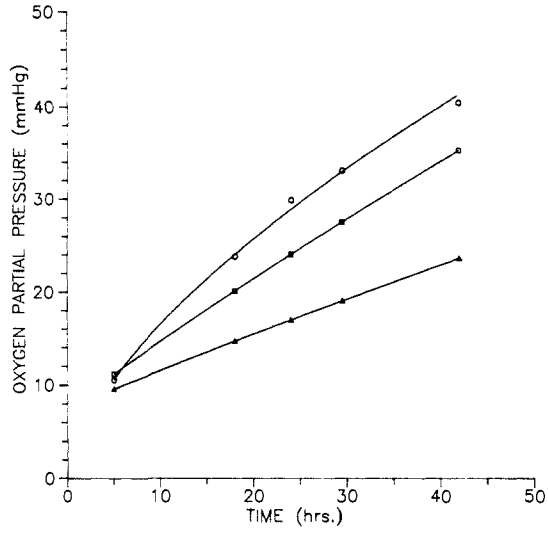

Figure 5. Plot of the partial pressure of oxygen in the lower chamber as a function of time: ○ = PS/[P]–CoSDPT (16.4%), □ = O_2 partial pressure expected for the cobalt-containing film (PS/[P]–CoSDPT, 16%) if no facilitated transport occurred (calculated by using the measured N_2 permeability coefficient from the cobalt film and the separation factor α ($\bar{P}_{O_2}/\bar{P}_{N_2}$) from the nickel blank), △ = partial pressure of O_2 if air permeated the cobalt membrane. A total pressure, X, was calculated from the measured P_{N_2} values using $0.79X = P_{N_2}$. The O_2 partial pressure expected from nonfacilitated transport is 21% of X.

pockets and filler aggregation, the nickel complexes are the best simulation for the unoxygenated cobalt-containing films and, therefore, are ideal blanks. Analysis of the polystyrene and nickel blanks is best made by observing the ratio of $\bar{P}_{O_2}$ to $\bar{P}_{N_2}$ and the separation factor, α, which describes the effectiveness of a membrane for permselectivity. The α values for both polystyrene and nickel blanks are reported in Table II.

To illustrate the enrichment that can be obtained by facilitated transfer, we have plotted the partial pressure of O_2 in the lower chamber as a function of time for the [P]–CoSDPT (16.4%) membrane (Figure 5). The change in N_2 partial pressure with time for this film is used as an internal standard to calibrate the permeation experiment. The average α value from the [P]–NiSDPT blanks is used to calculate the O_2 partial pressure corresponding to this N_2 pressure for an identical membrane in which facilitated transport does not occur and a first-order kinetic process is observed. Since the cobalt complex does not bind N_2 and facilitate its transport by a binding mechanism, this affords an ideal blank. This calculated pressure of O_2 is representative of all diffusion mechanisms other than facilitated transport and is also plotted as a function of time in Figure 5. The difference obtained between the curves represents the enrichment obtained by cobalt(II)-facilitated transport. Figure 5 also contains a reference curve in which no permselectivity is achieved; i.e., α = 1.00.

When the data are analyzed with the blank nickel α values and nitrogen permeability coefficients from the cobalt-containing membranes, systematic errors in measuring the enrichment of oxygen, particularly measurement of film thickness are cancelled out. This is verified experimentally with the nickel blanks themselves where α is seen to be independent of film thickness. We also find with the nickel data that percent loading and our variation in substituents on the phenyl ring do not influence the α values within the experimental standard deviation of +0.2. The reaction chamber can be evacuated after 25 h and the experiment cycled a second time with no change in α.

Table III contains the differences in partial pressures of oxygen between the cobalt-facilitated curves and back-calculated nonfacilitated curves, (as plotted in Figure 5), for a series of cobalt complex containing membranes. The differences were determined graphically at three different reaction times: when the back-calculated nonfacilitated partial pressure of oxygen, $P_{O_2}{}^B$, was 15, 20, and 25 Torr.

Table II. Separation Data for a Series of Polystyrene Blanks and Nickel Complexes

l, mm	Fl, Torr·mm/h	no. of pts[a]	α
Polystyrene Blanks			
First Cycle			
0.371 ± 0.073	1.7	3*F*	2.52 ± 0.02
0.542 ± 0.124	2.3	4*M*	1.37 ± 0.02
0.50 ± 0.00	3.4	6*F*	2.14 ± 0.02
0.164 ± 0.05	4.3	4*M*	1.40 ± 0.01
0.150 ± 0.052	1.5	4*M*	1.72 ± 0.01
0.250 ± 0.052	1.2	5*M*	2.19 ± 0.04
0.110 ± 0.028	1.0	7*F*	2.27 ± 0.02
0.131 ± 0.048	1.9	9*E*	2.34 ± 0.03
0.989 ± 0.16	5.4	5*F*	1.97 ± 0.05
1.567 ± 0.30	4.3	4*F*	2.76 ± 0.20
0.238 ± 0.051	1.5	3*M*	1.03 ± 0.16
av α = 1.97	SD =0.17		
Nickel Blanks			
wt %	l, mm	Fl, Torr·mm/h	no. of pts[a]	α
		[P]–NiSDPT		
		First Cycle		
20	0.457 ± 0.119	4.8	4*E*	1.79 ± 0.01
15	0.681 ± 0.059	3.1	5*M*	2.05 ± 0.02
10	0.423 ± 0.103	4.0	5*E*	1.57 ± 0.02
	av α = 1.80	SD = 0.17		
		[P]–NiBr2SDPT		
		First Cycle		
20	0.432 ± 0.12	3.9	5*E*	2.26 ± 0.03
20	0.700 ± 0.168	5.2	5*M*	1.80 ± 0.12
15	0.600 ± 0.160	3.0	6*M*	1.94 ± 0.06
10	0.628 ± 0.138	4.4	5*M*	1.79 ± 0.08
	av α = 1.95	SD = 0.13		
		Second Cycle		
25	0.709 ± 0.159	3.5	4*M*	2.12 ± 0.02
		[SG]–NiSDPT		
25	0.694 ± 0.105	4.5	5*M*	1.77 ± 0.05
20	0.666 ± 0.114	3.0	5*M*	1.73 ± 0.01
15	0.730 ± 0.079	4.7	4*M*	2.00 ± 0.04
	av α = 1.83	SD = 0.10		

[a] Number of data points in the data set. *E*, *M*, and *F* designate the time span of the experiment: *E*, <12 h; *M*, <29 h; *F*, >29 h.

The polymer-bound CoSDPT complex shows an enrichment of oxygen over the nonfacilitated process. The increasing amount of oxygen partial pressure at the three different reaction times can be explained by the variance in its permeation coefficient. Early on in the experiment, the oxygen permeation coefficient is largest, leading to an increase in the enrichment of P_{O_2}. Later in the experiment, the increased P_{O_2} value in the lower chamber approaches the $P_{1/2}$ value of the complex, and the facilitated transport of oxygen decreases. Eventually the cobalt complex is fully oxygenated and will not facilitate oxygen transport. No subsequent enrichment will occur; i.e., the experimental P_{O_2} curve and blank back-calculated curves become parallel (Figure 5). This is observed in all cases with the different cobalt complexes.

Second and third cycle experiments with [P]–CoSDPT produced similar enrichments in comparison with the original experiment. The fourth cycle showed a loss of enrichment presumably because of formation of a μ-peroxo complex or oxidation of the cobalt(II) complex. To confirm that the observed enrichment of O_2 was due in part to the reversible binding of O_2 and not just the desorption of O_2 from the complexes already formed during preparation of the membranes, the maximum amount of O_2 that could possibly be bound to the cobalt centers was calculated and observed to be considerably less than that observed in the permeation reactions.

Facilitated transport is also demonstrated for polymer-bound $CoBr_2$SDPT and Co3FSDPT with slightly higher enrichment

Table III. Partial Pressure Enrichment for a Series of Cobalt Complexes

wt %	l, mm	Fl, Torr·mm/h	P_{O_2} enrichment, Torr $P_{O_2}^B$ (15)	$P_{O_2}^B$ (20)	$P_{O_2}^B$ (25)
		[P]–CoSDPT			
		First Cycle			
44	0.261 ± 0.144	2.4	3.7	NA	NA
18.6	0.357 ± 0.065	2.6	1.0	2.5	2.6
16.4	0.687 ± 0.124	4.9	2.3	4.1	4.9
		av ΔP_{O_2}	2.3	3.3	3.8
		SD	1.0	1.1	1.6
		Second Cycle			
17.2	0.677 ± 0.044	5.1	4.2	5.0	5.9
16.4	0.687 ± 0.124	2.5	2.8	3.6	4.2
		av ΔP_{O_2}	3.5	4.3	5.0
		SD	1.0	1.0	1.2
		Third Cycle			
16.4	0.687 ± 0.124	2.9	2.6	3.2	3.6
		Fourth Cycle			
16.4	0.687 ± 0.124	4.4	−2.4	−3.5	−3.9
		[P]–CoBr2SDPT			
		First Cycle			
7.4	0.528 ± 0.072	3.7	2.9	3.9	4.0
6.76	0.671 ± 0.047	6.7	2.6	3.5	4.4
		av ΔP_{O_2}	2.8	3.7	4.2
		SD	0.2	0.3	0.3
		Second Cycle			
20.20	0.640 ± 0.051	5.8	−5.8	−4.5	−5.65
12.62	0.747 ± 0.074	3.7	−4.0	NA	NA
		av ΔP_{O_2}	−4.9	−4.5	−5.6
		SD	1.3		
		[P]–Co3FSDPT			
		First Cycle			
24.6	0.359 ± 0.050	2.3	6.0	7.1	7.9
16.47	0.506 ± 0.075	4.4	1.0	0.6	0.0
6.42	0.625 ± 0.085	5.9	3.0	4.0	4.4
6.30	0.541 ± 0.051	3.8	5.4	5.0	5.0
		av ΔP_{O_2}	3.8	4.2	4.3
		SD	1.3	1.6	1.9
		Second Cycle			
24.6	0.359 ± 0.050	1.4	−2.1	NA	NA
6.30	0.541 ± 0.051	2.4	0.5	1.0	1.3
		av ΔP_{O_2}	−0.8	1.0	1.3
		SD	1.8		
		[SG]–CoSDPT			
		First Cycle			
14.9	0.533 ± 0.097	5.6	1.0	2.1	2.5
10.0	0.807 ± 0.70	6.4	2.8	3.0	3.2
6.56	0.571 ± 0.082	4.8	1.6	1.5	0.9
4.6	0.614 ± 0.077	6.1	2.6	3.1	3.0
2	0.492 ± 0.028	4.9	1.3	2.6	2.6
		av ΔP_{O_2}	1.9	2.5	2.4
		SD	0.4	0.3	0.4
		Second Cycle			
16.5	0.647 ± 0.051	4.2	4.0	NA	NA
14.9	0.533 ± 0.097	3.2	2.5	3.2	2.5
10.0	0.807 ± 0.70	5.6	2.0	2.2	2.5
		av ΔP_{O_2}	2.8	2.7	2.5
		SD	0.7	0.7	0.0
		Lower Surface Studies			
16.1	0.384 ± 0.037	4.6	0.7	0.0	−0.5
1.87	0.358 ± 0.062	2.7	−1.0	−1.6	−1.5
		av ΔP_{O_2}	−0.2	−0.8	−1.0
		SD	1.2	1.1	0.7

values. However, in these cases the second cycle no longer showed any enhancement, again presumably because of formation of a

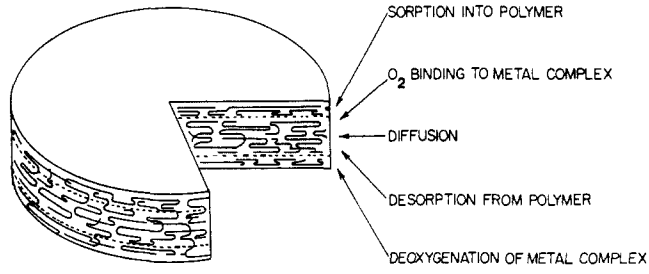

Figure 6. Contributions to oxygen permeation in supported cobalt complex containing membranes.

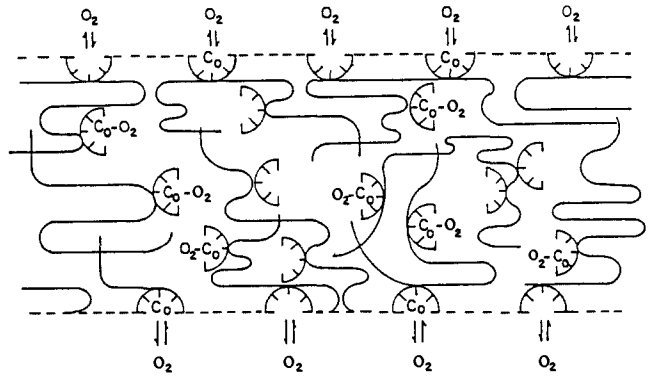

Figure 7. Cobalt complex facilitated transport of oxygen via a site to site interaction.

μ-peroxo complex or oxidation of the cobalt(II) complex. When CoSDPT was covalently attached to silica gel (0.5 mmol/g) and added to a polystyrene membrane, a smaller degree of enrichment was obtained.

The mechanism of O_2 transport involved in the membranes described above is unlike that in liquid membranes. For O_2 permeation using supported metal complexes in solid polymer membranes, at least five individual processes are involved. These are shown in Figure 6. They include the nonfacilitated process, which involves solubility of the gas, diffusion, and desorption from the polymer. The facilitated path also involves O_2 binding to the metal complex, O_2 transfer to cobalt sites through the polymer, and deoxygenation of the metal complex. On the high-pressure side, the attainment of equilibrium for O_2 solubility at the polymer interface is an exothermic process, as is dioxygen binding to the metal center. These are not viewed as rate determining in the transport process. The importance of the metal center in the diffusion process is much more complex. It is proposed that the cobalt complexes transport O_2 via a site to site transfer (Figure 7). The O_2 bound to cobalt is in equilibrium with O_2 that is soluble in the polymer, maintaining a reservoir of free O_2 through the film. Cobalt–oxygen complexes on the low-pressure side dissociate O_2 into the gas phase and replace it by binding O_2 from a neighboring reservoir. This would necessitate a dispersion of the oxygen carriers throughout the membrane as opposed to having them only on the lower surface. The latter configuration showed no O_2 enrichment experimentally (Table III, Lower Surface Studies).

Conclusion

In conclusion, we have developed a procedure for ascertaining facilitated transfer of oxygen that in effect uses the permeation of nitrogen in the sample membrane as an internal standard. By so doing, we have demonstrated that supported cobalt complexes incorporated into a polystyrene membrane enhance the permeation of dioxygen. Having accomplished these objectives, further work will involve extension of these experiments to higher cobalt(II) loading and to rubbery polymers. The mechanism of facilitated transport in this system differs from that in liquid membranes where diffusion of the entire complex can carry O_2 across the membrane. A site to site transfer is proposed here, and this

mechanism requires that some of the cobalt be deoxygenated in the membrane. The $P_{1/2}$ value for CoSDPT in solution is reported[14] to be 6.715×10^3 mmHg at 295 K. A more stable adduct forms in the polymer,[15] and its $P_{1/2}$ value determines the partial pressure of O_2 that can be attained on the lower pressure side before metal-facilitated enhancement ceases.

Acknowledgment. This research was supported by the Army CRDEC through the University of Florida Technology Center and the National Science Foundation (Grant 86 18766).

Registry No. O_2, 7782-44-7; polystyrene, 9003-53-6.

(14) Drago, R. S.; Cannady, J. P.; Leslie, K. A. *J. Am. Chem. Soc.* **1980**, *102*, 6014.
(15) Drago, R. S.; Gaul, J. H. *Inorg. Chem.* **1979**, *18*, 2019.

Some Thermal and Photochemical Reactions of [4.4.4.5]Fenestranes

Steven Wolff,[1a,b] Bhaskar Rao Venepalli,[1a,c,d] Clifford F. George,[1e] and William C. Agosta*,[1a]

Contribution from the Laboratories of The Rockefeller University, New York, New York 10021-6399, and Laboratory for the Structure of Matter, Naval Research Laboratory, Washington, D.C. 20375-5000. *Received February 16, 1988*

Abstract: Thermolysis of **8b** at 100 °C in benzene leads to isomerization to **12** and **14**, and **9b** furnishes **13** rather than **12**. Products **12** and **13** are regarded as resulting from a concerted $[{}_\pi 2_s + {}_\pi 2_s + {}_\pi 2_s]$ cycloreversion. In methanol **14** is replaced by solvent adduct **20**, and it is suggested that both **14** and **20** are secondary products resulting from further reaction of initially formed **16**. Photolysis of **8b** ($\lambda > 280$ nm) in benzene containing methanol gives small amounts of **20** and **21**, along with aldehyde **28**. The former arise through β-cleavage of the ketone, and **28** results from α-cleavage, followed by bond scission and hydrogen transfer. Mechanistic explanations for these various reactions are supported by both molecular mechanics and MNDO calculations. Formation of these products demonstrates the role of the short, weak bonds to the central carbon atom C(10) in controlling reactions of these [4.4.4.5]fenestranes.

One incentive for preparation of novel strained systems is the opportunity to assess the effects of their structures on chemical transformations. For derivatives of [4.4.4.5]fenestrane (**1**), both

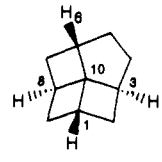

1

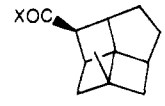

2a, X = *p*-BrC_6H_4NH
b, X = CH_3O

MNDO calculations[2] and the crystallographic structure of **2a**[3] indicate that the bond angles at the central quaternary carbon C(10) are opened from the normal value of ~109° to 128–129° and that bonds to this atom are unusually short, averaging 1.508 Å.[4] Keese has pointed out that, among systems with increased sp^3 bond angles, the fenestranes are essentially unique in that these changes occur almost solely through compression and involve little or no twisting.[5] We have now examined transformations in [4.4.4.5]fenestranes for evidence for the chemical effects of this skeletal distortion and report here studies of photolysis and thermolysis in this series. The results reveal a significant role in these reactions for the short, weak bonds to the central carbon atom of these compounds. In previous studies,[2] semiempirical MNDO calculations have provided rather accurate structural parameters for several fenestrane systems, and with this in mind we have employed both MNDO and molecular mechanics procedures as an aid in guiding and interpreting various aspects of this work.

Scheme I[a]

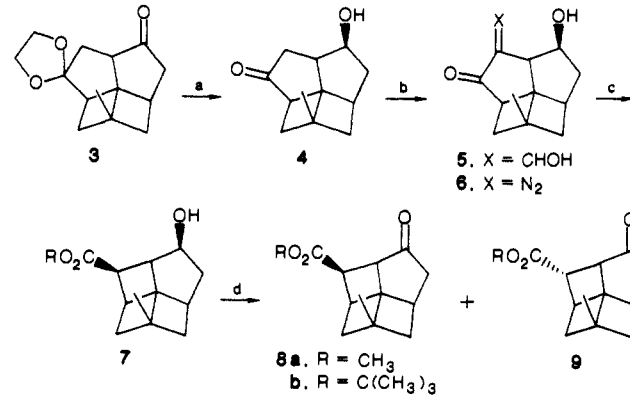

[a] Key: (a) $LiAlH_4$; TsOH, H_2O; (b) HCO_2Et, CH_3O^-;[3,7] **5**, MsN_3, Et_3N;[3,8,9] (c) **6**, *hν*, ROH;[3,10] (d) $OxCl_2$, DMSO, Et_3N.[11]

Preparation of the desired substrates proceeded as detailed in Scheme I, starting with the previously described[3] keto ketal **3**. The structure of major (~10:1) reduction product **4** was assigned as shown since in models of **3** approach of hydride to the carbonyl group appears less hindered from below; rigorous proof for this stereochemistry comes from an X-ray structure noted below.[6] As

(1) (a) The Rockefeller University. (b) Current address: Chemical Research Department, Hoffmann-La Roche, Inc., Nutley, NJ 07110. (c) Formerly V. Bhaskar Rao. (d) Current address: Life Sciences Research Laboratory, Eastman Kodak Co., Rochester, NY 14650. (e) Naval Research Laboratory.
(2) Keese, R.; Luef, W., unpublished results. Luef, W. D. *Inauguraldissertation*, Universität Bern, Berne, Switzerland, 1985.
(3) Rao, V. B.; George, C. F.; Wolff, S.; Agosta, W. C. *J. Am. Chem. Soc.* **1985**, *107*, 5732.
(4) A general review, including a discussion of nomenclature, is available: Venepalli, B. R.; Agosta, W. C. *Chem. Rev.* **1987**, *87*, 399. In the present work [4.4.4]fenestrane refers to tricyclo[4.2.0.$0^{1,4}$]octane, [4.4.5.5]fenestrane to (1,11-*syn*,1α,3β,6α,9β)tetracyclo[4.4.1.$0^{3,11}$.$0^{9,11}$]undecane, and [4.4.4.5]-fenestrane to (1,10-*syn*,1α,3β,6α,8β)tetracyclo[4.3.1.$0^{3,10}$.$0^{8,10}$]decane.
(5) Luyten, M.; Keese, R. *Tetrahedron* **1986**, *42*, 1687. Luef, W.; Keese, R. *Helv. Chim. Acta* **1987**, *70*, 543.
(6) Selective formation of **4** is in contrast with the behavior of *cis*-bicyclo[3.3.0]octan-2-one, where reduction with hydride reagents under a variety of conditions yields largely the endo alcohol: Fujita, K.; Hata, K.; Oda, R.; Tabushi, I. *J. Org. Chem.* **1973**, *38*, 2640.

0002-7863/88/1510-6785$01.50/0